ChemComm

Accepted Manuscript

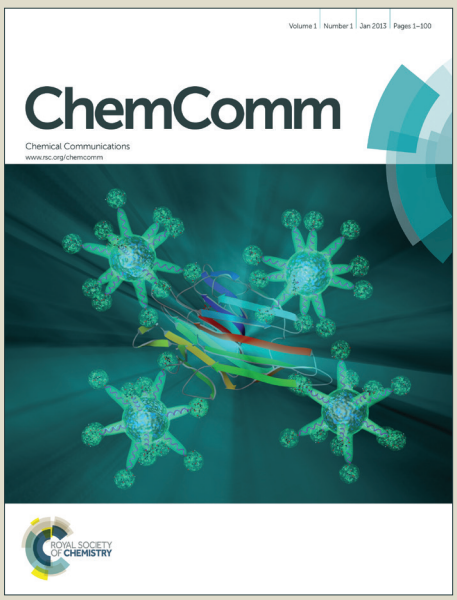

ROYAL SOCIETY OF CHEMISTRY

www.rsc.org/chemcomm

Chemical Communications RSCPublishing

COMMUNICATION

Efficient Electrochemiluminescence of a boron-dipyrromethene (BODIPY) dye

Cite this: DOI: 10.1039/x0xx00000x

Mahdi Hesari, [a‡] Jia-sheng Lu, [b,c‡] Suning Wang,* [b,c] and Zhifeng Ding*[a]

Received ooth January 2012,
Accepted ooth January 2012

DOI: 10.1039/x0xx00000x

www.rsc.org/

Electrochemiluminescence (ECL) of a boron-dipyrromethene dye (BDY) in the presence of tri-*n*-propylamine as a co-reactant was found to be highly efficient. The ECL of BDY showed a unique peak wavelength of 707 nm, indicative of intermolecular electronic transition mechanism.

Boron-dipyrromethene (BODIPY) dye family covers a wide range of so-called supermolecular compounds, which are well-known for their specific absorption and emission optical properties.[1] Importantly, these optical features can be altered feasibly *via* structural modifications at the different BODIPY core positions (see Scheme 1),[2, 3] where different derivatives display diverse colours in solution.[4-6] The BODIPY dyes mostly show peculiarly high absorption coefficient and photoluminescence quantum efficiency in both visible and near-infrared (NIR) regions due to the electron rich core. Thus, BODIPY dyes are anticipated to be useful indicators and biomarkers in biological studies.[4, 7, 8] In addition to the optical properties, BODIPY dyes possess diverse electrochemical features, which also depend on their structural design.[9, 10] Therefore, BODIPY dyes with a wide range of modification or functionalization have been used in photoelectrochemical studies including photo-induced energy transfer (PET),[11, 12] photovoltaic devices,[13-17] and electrogenerated chemiluminescence (ECL) process.[18, 19] ECL is an important photoelectrochemical technique with a diverse applications in both fundamental and analytical aspects for organic and inorganic martials.[20-28] Bard and co-workers are pioneer in studying various BODIPY dyes as ECL emitters.[29] They showed that the structural properties play an important role in the ECL emission wavelength and efficiency.[9, 30-34] Here, ECL of a giant BOPIDY dye (abb. as BDY, Scheme 1) including a biphenyl linker and two long chain (C8) arms in the *meso* and *alpha* positions[13] was investigated. Essentially, the presence of the aromatic chains provides a high possibility for π interaction, which provides a feasible route for intermolecular electronic transition. Blocking at *alpha*, *beta* or *meso* positions of the BODYPY core is expected to stabilize the electrogenerated radicals needed to generate the excited state, and therefore to enhance the ECL intensity. The ECL efficiency of BDY showed a remarkable increase relative to the other BODIPY dyes. The ECL mechanisms were correlated to the electrochemistry and structure of the dye. For the first time, the Latimer-type diagram was obtained for the BODIPY dye to connect photochemical and electrochemical features.

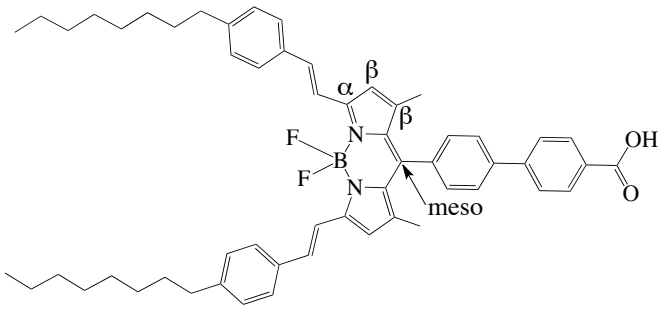

Scheme 1. Molecular structure of the BDY.

The synthesis of the BDY dye was reported elsewhere.[13] Figure 1A shows the spooling ECL spectra of 0.4 mM BDY in the presence of 20 mM tri-*n*-propylamine (TPrA) in CH_2Cl_2 containing 0.1 M tetra-*n*-butylammonium hexafluorophosphate ($TBAPF_6$) as the supporting electrolyte at a scan rate of 20 mVs^{-1}. The spectra were acquired along with a potential scanning cycle between 0.0 and 1.4 V *vs.* SCE. It can be noticed that the onset ECL spectrum recorded at 0.700 V *vs.* SCE has a peak wavelength of 707 nm. At this potential the BDY dye was already oxidized to the corresponding radical cation ($BDY^{\bullet+}$) (Figure 2, Ox_1, $E^{o'}$= 0.603 V). At a very close potential (0.810 V *vs.* SCE[35]), TPrA was also oxidized to its radical cation intermediate ($TPrA^{\bullet+}$), which deprotonated to form TPrA radical ($TPrA^{\bullet}$) with a highly reductive power (E°= -1.7 V),[35, 36] Scheme 2. The electrogenerated $BDY^{\bullet+}$ and $TPrA^{\bullet}$ met in the vicinity of the working electrode, where a single electron transfer from HOMO of the $TPrA^{\bullet}$ to the LUMO of the $BDY^{\bullet+}$ dye occurred. As a result, an excited state of the BDY (BDY*) formed,

COMMUNICATION

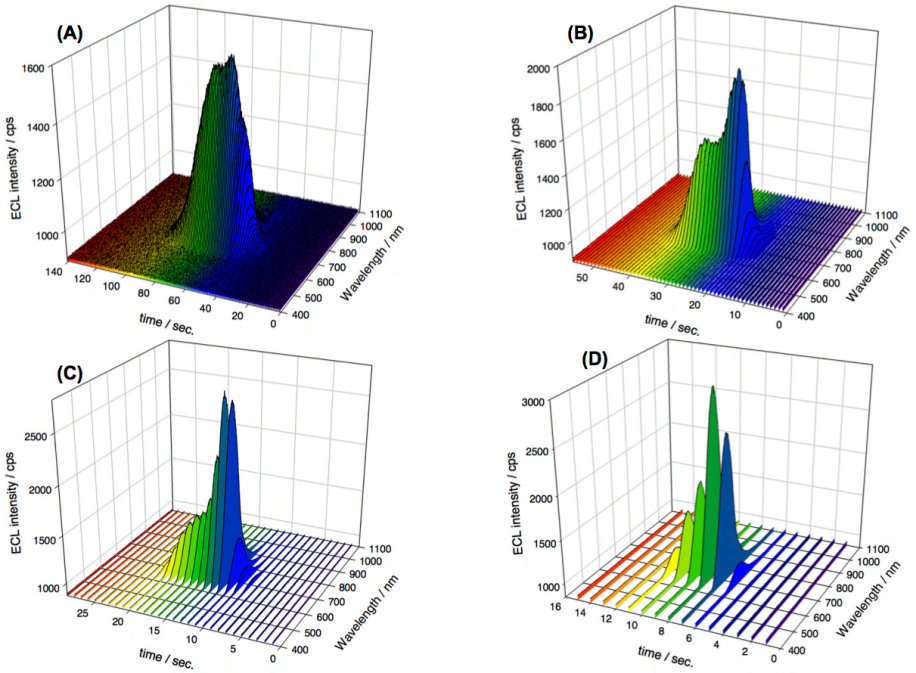

Figure 1. Spooling ECL spectra of 0.4 mM BDY /20 mM TPrA in CH_2Cl_2 containing 0.1 M $TBAPF_6$ during a potential scanning cycle between 0.0 and 1.4 V at (A) 20, (B) 50, (C) 100, and (D) 200 mVs^{-1}. Each spectrum was acquired for 1 s interval.

which relaxed to the ground state and fluoresced at 707 nm, Scheme 2. Scanning potential towards the more positive values generated more $TPrA^{\bullet}$, which increased the [BDY*] and lead to the ECL evolution (Figure 1 A). The ECL emission reached to the first maximum at t= 51 sec. (1.020 V), while the ECL emission remained at 707 nm. At higher positive potential the second maximum was recorded at t=59 sec. (1.180 V). BDY underwent the second oxidation at 1.075 V (Figure 2, Ox_2) to generate BDY dication (BDY^{2+}), which reacted with BDY in the solution to produce two $BDY^{\bullet+}$, Scheme 2. Due to the increased [$BDY^{\bullet+}$], the ECL intensity was enhanced as demonstrated by the second maximum in the spooling spectra. Obviously, the second maximum was attributed to the emission from the same excited state, BDY*. Upon scanning the potential further positive and in the reverse direction, the ECL intensity decreased due to the depletion and reverse conversion of the $TPrA^{\bullet}$ and BDY species. The ECL evolution and devolution pattern demonstrated from the spooling spectroscopy is matched by that from the ECL-voltage curve shown in Figure S1A-B.

The ECL dependence of the BDY/TPrA system on the scan rate was investigated by means of spooling spectroscopy at potential scan rates of 50, 100 and 200 mVs^{-1}, respectively, Figure 1B-D. In all cases, the same ECL peak wavelength was observed. The higher the scan rate, the greater the ECL intensity in the spooling spectra for a time interval of 1 s. It is interesting to note that the opposite trend can be see by comparing accumulated ECL spectra obtained during two potential scanning cycles between 0 and 1.4 V at different scan rates (Figure S2). The BDY^{2+} decay and the amount of charged BDY species produced in the ECL process are the two competing factors. The BDY^{2+} stability was the dominant in short term; therefore fast scan rate favoured the $BDY^{\bullet+}$ production and therefore the high ECL intensity in the spooling spectra. In contrast, the large amount of charged BDY species produced at the slow scan rates lead to high intensity in the long term accumulated ECL spectra.

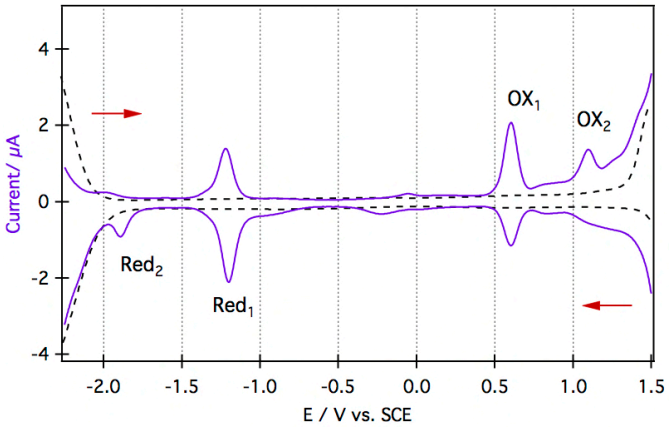

Figure 2. Differential pulse voltammograms (DPVs) of 0.4 mM BDY dye in dichloromethane containing 0.1 M $TBAPF_6$ (solid) and the blank electrolyte (dashed).

Shown in Figure 3 (dashed-line) is the photoluminescence (PL) spectrum of 0.01 mM of BDY in CH_2Cl_2 recorded with the same camera and a 532 nm laser for excitation. Two peaks at 604 nm (2.05 eV) and at 692 nm (1.79 eV) can be determined by curve-fitting the spectrum (Figure S3), which are in line with those in toluene reported by one of our groups.[13] While the PL of BODIPY dyes is known to be weakly influenced by the solvent,[37, 38] the longer wavelength peak red-

shifted further in this high concentration is attributed to an intermolecular electronic transition process, BDY aggregation. The shorter one is due to the relaxed excited state across the HOMO-LUMO gap. In contrast, the accumulated ECL peak wavelength over two cycles of potential scanning between 0 and 1.4 V shows a single peak at 707 nm (1.75 eV), Figure 3. Thus, it is plausible that the intermolecular electronic transition is dominant in the ECL processes.

The ECL of the 0.4 mM BDY electrolyte solution was measured (Figure S4) upon continuous alternative electrochemical oxidation and reduction between the potentials defined by the DPVs in Figure 2. No appreciable ECL via this annihilation path can be observed, where electrogenerated $BDY^{\bullet+}$ and $BDY^{\bullet-}$ was expected to react for the emissive BDY* generation. The ECL was enhanced dramatically when the working electrode was quickly pulsed between -1.5 to 0.8 V (first reduction and oxidation peak potentials) with a pulse width of 0.1 s (Figure S5). The ECL intensity at 0.5 V is much larger than that at -1.5 V, indicating a higher stability of $BDY^{\bullet-}$ than that of $BDY^{\bullet+}$. ECL peak wavelength in the accumulated spectrum (Figure S5) was found to be 707 nm as well.

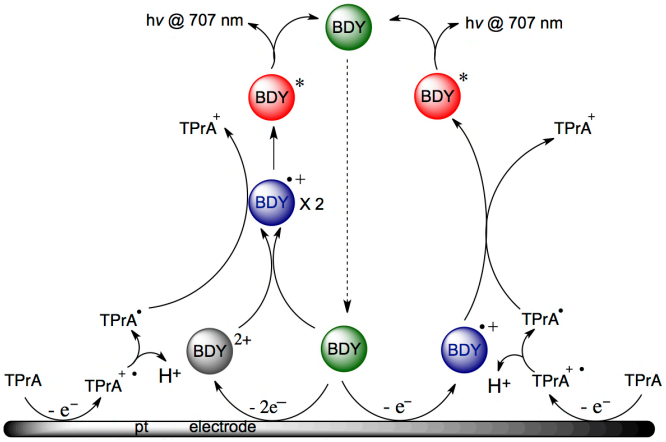

Scheme 2. Proposed ECL mechanisms of BDY/TPrA system.

Table 1. ECL efficiency dependence of the BDY/TPrA system on scan rates.

Scan rate mV/s	PMT ECL eff. %	Camera ECL eff.%
20	81	97
50	72	58
100	70	60
200	69	63

The ECL efficiency, φ_{ECL}, of BDY/TPrA system was measured as the photons emitted per redox event relative to that of $Ru(bpy)_3^{2+}$/TPrA.[39] ECL-voltage curves and cyclic voltammograms of the two systems in the same conditions were used to calculate the amount of photons and electrons, Table 1 and ESI. The BDY/TPrA system reached a relative efficiency of 81% at a potential scan rate of 20 mVs^{-1}. The ECL efficiency was also determined by means of the ratio of photons under an ECL spectrum accumulated during 2 cycles of potential scan to the charge integrated from the corresponding voltammogram. In this way, the relative φ_{ECL} shows a value of almost 100% for the BDY/TPrA at the same scan rate, Table 1. The response of the camera to BDY/TPrA (707 nm) and $Ru(bpy)_3^{2+}$/TPrA (610 nm) ECL emissions has a quantum efficiency of 90 and 80 % (Figure S6), respectively, while the R928 photomultiplier tube used for the ECL-voltage curves has a sensitivity of 30 and 45 mA/W (Figure S7) for the two wavelengths, respectively. Thus the relative φ_{ECL} in the light generation process at 20 mVs^{-1} should be between 80 and 100%. Table 1 also shows the ECL efficiency dependence on scan rates. In general, the lower the scan rate, the higher the charge injection to the elecroactive species. This eventually resulted in more ECL light emission, a consequence of the combined kinetic and thermodynamic process involved in the ECL generation.

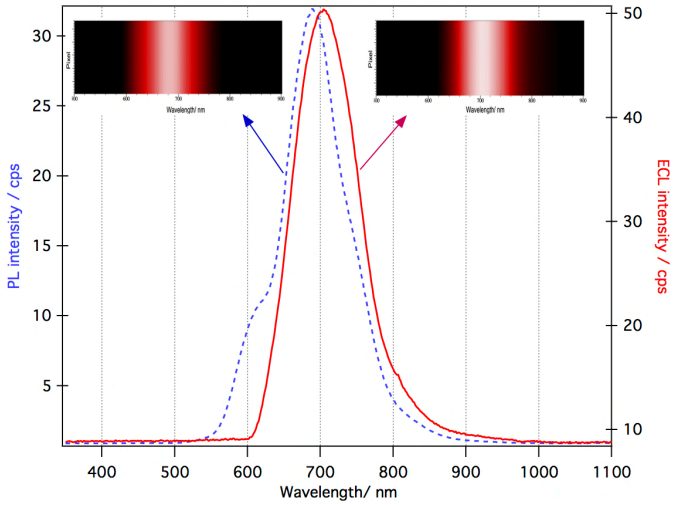

Figure 3. Photoluminescence (blue dashed-line) and accumulated ECL (red solid) spectra of BDY in CH_2Cl_2. The insets show the corresponding PL (top-left) and ECL(top-right) spectrum image on the CCD camera.

The electrochemical energy gap of the BDY was calculated to be 1.82 eV from the formal potentials of Ox_1 and Red_1, which is smaller than the ones for a series of BODIPY dyes with different structures (2.43-1.58 eV).[29] Electronically, the two oxidation reactions (Ox_1 and Ox_2 in Figure 2) were probably localized in the BDY core and its π conjugation branches at α positions as illustrated by the HOMO from the DFT calculation, Figure S8. The presence of the conjugated system through the BDY structure leads to the stabilization of the electrogenerated radical anions and cations,[29] which likely enhance the ECL efficiency.

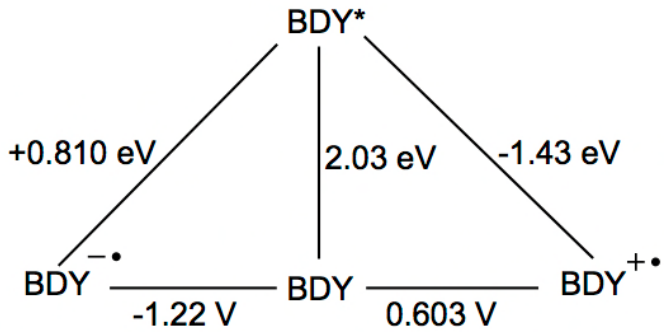

Scheme 3. Latimer-type diagram for BDY.

A Latimer-type diagram can be used to correlate electrochemical and photochemical features of various BDY species.[40, 41] Based on the electrochemical and PL spectroscopy data, we obtained the Latimer-type diagram for BDY as shown in Scheme 3. To our best knowledge this is the first report on the Latimer-type diagram of such systems. The thermodynamics confirms that TPrA is a suitable co-reactant for the BDY ECL generation: the $TPrA^{\bullet}$ possesses high reduction power (-1.7 eV), which is enough to inject electron to the $BDY^{\bullet+}$ (-1.2 eV) for the generation of BDY excited state BDY* in the ECL process.

In summary, the ECL of BDY has been examined in the presence of TPrA as a co-reactant. Spooling ECL spectra displayed a peak wavelength of 707 nm, revealing the dominance of intermolecular electron transition. Along with the conventional ECL-voltage curve method, light generation at low scan rate has revealed two emission maxima involving the electron transfer between the electrogenerated $TPrA^{\bullet}$ and $BDY^{\bullet+}$ at 1.02 V, and between the $TPrA^{\bullet}$ and concentration-enhanced $BDY^{\bullet+}$ via a reaction of BDY^{2+} with BDY at 1.18 V. The stable ECL has reached an efficiency as high as 100% relative to $Ru(bpy)_3^{2+}$ at a potential scan rate of 20 mVs^{-1}, demonstrating the feasibility of BDY as an efficient dye for ECL. For the first time Latimer-type diagram has been constructed for such a dye system, illustrating the thermodynamic origin of the ECL system.

This work was financially supported by NSERC, CFI, PREA, Western and Queen's. Quality service from the Electronic Shop and ChemBio Store in Chemistry at Western is appreciated.

Notes and references

[a] Department of Chemistry, The University of Western Ontario, London, ON N6A 5B7, Canada, zfding@uwo.ca .

[b] Department of Chemistry, The Queen's university, Kingston, ON K7L 3N6, Canada, wangs@chem.queensu.ca .

[c] Beijing Key Laboratory of Photoelectronic/Electrophotonic Conversion Materials, School of Chemistry, Beijing Institute of Technology, Beijing 100081, P.R. China.

‡ These authors contributed equally.

† Electronic Supplementary Information (ESI) available: Experimental detail, ECL-voltage curve of BDY in the course of annihilation, spooling ECL peak intensity-voltage curve of BDY/TPrA at scan rate of 20 mVs^{-1}, Accumulated ECL spectra at different scan rates, Curve-fitted PL spectrum, ECL in potential scanning and pulsing experiments via the annihilation path and the corresponding ECL spectrum, ECL efficiency calculations, iDus CCD camera and R928 PMT response curves, and HOMO-LUMO orbitals of BDY dye. See DOI: 10.1039/c000000x/

1. A. Bessette and G. S. Hanan, *Chem. Soc. Rev.*, 2014, **43**, 3342-3405.
2. L. Li, J. Han, B. Nguyen and K. Burgess, *J. Org. Chem.*, 2008, **73**, 1963-1970.
3. A. Loudet and K. Burgess, *Chem. Rev.*, 2007, **107**, 4891-4932.
4. N. Boens, V. Leen and W. Dehaen, *Chem. Soc. Rev.*, 2012, **41**, 1130-1172.
5. X. Zhu, R. Liu, Y. Li, H. Huang, Q. Wang, D. Wang, X. Zhu, S. Liu and H. Zhu, *Chem. Commun.*, 2014, **50**, 12951-12954.
6. Y. Wang, L. Chen, R. M. El-Shishtawy, S. G. Aziz and K. Mullen, *Chem. Commun.*, 2014, **50**, 11540-11542.
7. A. Vázquez-Romero, N. Kielland, M. J. Arévalo, S. Preciado, R. J. Mellanby, Y. Feng, R. Lavilla and M. Vendrell, *J. Am. Chem. Soc.*, 2013, **135**, 16018-16021.
8. A. Barba-Bon, A. M. Costero, S. Gil, F. Sancenon and R. Martinez-Manez, *Chem. Commun.*, 2014.
9. A. B. Nepomnyashchii, S. Cho, P. J. Rossky and A. J. Bard, *J. Am. Chem. Soc.*, 2010, **132**, 17550-17559.
10. V. Engelhardt, S. Kuhri, J. Fleischhauer, M. Garcia-Iglesias, D. Gonzalez-Rodriguez, G. Bottari, T. Torres, D. M. Guldi and R. Faust, *Chem. Sci.*, 2013, **4**, 3888-3893.
11. C. Y. Lee and J. T. Hupp, *Langmuir*, 2009, **26**, 3760-3765.
12. E. M. Sanchez-Carnerero, L. Gartzia-Rivero, F. Moreno, B. L. Maroto, A. R. Agarrabeitia, M. J. Ortiz, J. Banuelos, I. Lopez-Arbeloa and S. de la Moya, *Chem. Commun.*, 2014, **50**, 12765-12767.
13. J.-s. Lu, H. Fu, Y. Zhang, Z. J. Jakubek, Y. Tao and S. Wang, *Angew. Chem. Int. Ed.*, 2011, **50**, 11658-11662.
14. S. P. Singh and T. Gayathri, *Eur. J. Org. Chem.*, 2014, **2014**, 4689-4707.
15. Y. Ooyama, Y. Hagiwara, T. Mizumo, Y. Harima and J. Ohshita, *RSC Adv,*, 2013, **3**, 18099-18106.
16. Y. Ooyama, Y. Hagiwara, T. Mizumo, Y. Harima and J. Ohshita, *New J. Chem.*, 2013, **37**, 2479-2485.
17. B. Kim, B. Ma, V. R. Donuru, H. Liu and J. M. J. Frechet, *Chem. Commun.*, 2010, **46**, 4148-4150.
18. A. Venkatanarayanan, A. Martin, K. M. Molapo, E. I. Iwuoha, T. E. Keyes and R. J. Forster, *Electrochem. Commun.*, 2013, **31**, 116-119.
19. A. Venkatanarayanan, A. Martin, T. E. Keyes and R. J. Forster, *Electrochem. Commun.*, 2012, **21**, 46-49.
20. A. J. Bard, *Electrogenerated Chemiluminescence*, Marcel Dekker, 2004.
21. W. Miao, *Chem. Rev.*, 2008, **108**, 2506-2553.
22. M. M. Richter, *Chem. Rev.*, 2004, **104**, 3003-3036.
23. Z. Ding, B. M. Quinn, S. K. Haram, L. E. Pell, B. A. Korgel and A. J. Bard, *Science*, 2002, **296**, 1293-1297.
24. C. Booker, X. Wang, S. Haroun, J. Zhou, M. Jennings, B. L. Pagenkopf and Z. Ding, *Angew. Chem. Int. Ed.*, 2008, **47**, 7731-7735.
25. M. Hesari, M. S. Workentin and Z. Ding, *ACS Nano*, 2014, **8**, 8543-8553.
26. M. Hesari, M. S. Workentin and Z. Ding, *Chem. Sci.*, 2014, **5**, 3814-3822.
27. K. N. Swanick, M. Hesari, M. S. Workentin and Z. Ding, *J. Am. Chem. Soc.*, 2012, **134**, 15205-15208.
28. P. Wu, X. Hou, J.-J. Xu and H.-Y. Chen, *Chem. Rev.*, 2014, DOI: 10.1021/cr400710z.
29. A. B. Nepomnyashchii and A. J. Bard, *Acc. Chem. Res.*, 2012, **45**, 1844-1853.
30. A. B. Nepomnyashchii, A. J. Pistner, A. J. Bard and J. Rosenthal, *J. Phys. Chem. C*, 2013, **117**, 5599-5609.
31. J. Rosenthal, A. B. Nepomnyashchii, J. Kozhukh, A. J. Bard and S. J. Lippard, *J. Phys. Chem. C*, 2011, **115**, 17993-18001.
32. A. B. Nepomnyashchii, M. Bröring, J. Ahrens and A. J. Bard, *J. Am. Chem. Soc.*, 2011, **133**, 19498-19504.
33. A. B. Nepomnyashchii, M. Broering, J. Ahrens, R. Krueger and A. J. Bard, *J. Phys. Chem. C*, 2010, **114**, 14453-14460.
34. H. Qi, J. J. Teesdale, R. C. Pupillo, J. Rosenthal and A. J. Bard, *J. Am. Chem. Soc.*, 2013, **135**, 13558-13566.
35. R. Y. Lai and A. J. Bard, *J. Phys. Chem. A*, 2003, **107**, 3335-3340.
36. M. Hesari, M. S. Workentin and Z. Ding, *RSC Adv,*, 2014, **4**, 29559-29562.
37. D. Kajiya, K. Nishikawa and K.-i. Saitow, *J. Phys. Chem. A*, 2005, **109**, 7365-7370.
38. W. Qin, T. Rohand, M. Baruah, A. Stefan, M. V. der Auweraer, W. Dehaen and N. Boens, *Chem. Phys. Lett.*, 2006, **420**, 562-568.
39. C. Booker, X. Wang, S. Haroun, J. Zhou, M. Jennings, B. L. Pagenkopf and Z. Ding, *Angew. Chem. Int. Edit.*, 2008, **47**, 7731-7735.
40. H. B. Gray and A. W. Maverick, *Science*, 1981, **214**, 1201-1205.
41. M. Hesari, M. S. Workentin and Z. Ding, *Chem. Eur. J.*, 2014, **20**, 15116-15121.

